

Two-photon excitation 4Pi confocal microscope: Enhanced axial resolution microscope for biological research

P. E. Hänninen, S. W. Hell,^{a)} J. Salo, and E. Soini

Department of Medical Physics, University of Turku and Centre for Biotechnology, Tykistökatu 6, SF-20520 Turku, Finland

C. Cremer

Institut für Angewandte Physik, Universität Heidelberg, D-69120 Heidelberg, Germany

(Received 6 December 1994; accepted for publication 1 February 1995)

The applicability of two photon excitation 4Pi confocal fluorescence microscopy to biological imaging is demonstrated. We show that 4Pi confocal microscopy in combination with a simple deconvolution algorithm allows axial localization and quantification with 0.14 μm resolution in a biological sample. The 4Pi-confocal microscope extends the applicability of far field fluorescence microscopy to high resolution three-dimensional imaging and quantification of subcellular structures.

Three-dimensional (3D) imaging of specimen is important for the quantitative study of transparent objects in microscopy. Light microscopy offers a nondestructive way of studying 3D structures within the specimen. Therefore scanning light microscopies are of increasing importance for the elucidation of structure and function of subcellular organelles. One of the major limitations of these techniques is the diffraction limited resolution which is determined by the wavelength of light and the numerical aperture of the lens. The resolution limitation is most evident along the optical axis, where the typical limits are 500 nm. Axial structures smaller than 500 nm cannot be resolved.

A promising method for increasing the axial resolution is 4Pi-confocal microscopy. In a 4Pi confocal microscope, two opposing objective lenses are coherently used for illuminating or detecting the same object point.¹⁻⁴ When both lenses are illuminated simultaneously and the counter propagating wave fronts interfere in the common focus the intensity distribution is given by the interference pattern of two counter propagating spherical wave fronts (type-A 4Pi confocal microscopy). If the wave fronts are in phase at the geometrical focus, the illumination intensity distribution or illumination point-spread-function (PSF) consists of a main peak and two axial lobes on each side. With strong axial lobes the axial resolution is not increased, unless the lobes are taken into account mathematically. This is even more important for the non-scanning standing wave microscope,⁵⁻⁷ a further approach to increase the axial resolution where two flat wave fronts form an interference pattern across the whole field with several lobes of comparable height.

Based on a high aperture vectorial theory, one can calculate that for an aberration-free system the axial lobes almost vanish in a 4Pi confocal fluorescence microscope using two-photon excitation.² This is due to the quadratic intensity dependence of two-photon excitation and the narrow spatial filtering of the confocal detection pinhole. In practice, however, the axial lobes are higher than what is found in theory. The reasons are shortcomings of high aperture theories^{8,9} as

well as aberrations introduced by the optical elements and the sample. It is therefore interesting to investigate the imaging behavior of a two-photon excitation 4Pi confocal microscope in a real biological sample and to develop methods for exploiting the full resolution potential of 4Pi confocal microscopy.

We constructed a two-photon excitation 4Pi confocal microscope using a pulsed femtosecond titanium-sapphire laser (Coherent Mira 900F) for excitation (Fig. 1). High numerical aperture objectives (1.4 oil) and tube lenses from a recently developed microscope with advanced aberration correction were chosen (Leitz DM microscope, Leitz PL APO 0.7-1.4). The sample was mounted between two cover slips and attached to a piezoelectric stage (Physik Instrumente PI F603.00) scanning the sample with an accuracy of 10 nm at the common focus of the lenses.

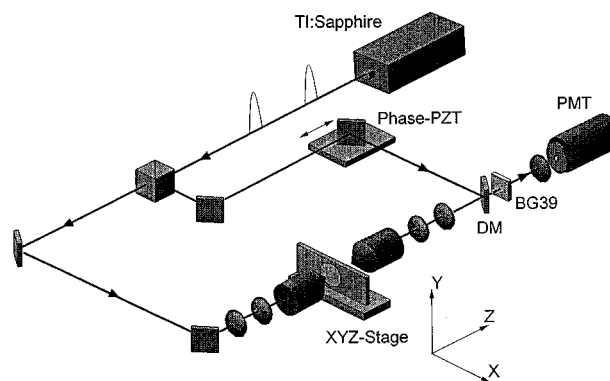


FIG. 1. Two-photon 4Pi confocal setup: The sample is mounted between two cover slips and attached to a precision XYZ-scanning stage (Lightline, Physik Instrumente, Inc.). The stage is capable of positioning the sample with an accuracy of 10 nm in all three directions. Two opposing lenses of high numerical aperture (Leitz, DM, APO PL 1.4, oil) focuses the light to the same point inside the sample. For two-photon excitation a mode-locked Ti:sapphire laser (Mira 900F, Coherent, Inc.) providing with a stream of 130 fs pulses with a repetition rate of 76 MHz is used. The pulses are split and guided along two paths of equivalent length to ensure interference in the common focus of the lenses. The relative phase of the wave fronts is adjusted by a piezoelectrically driven mirror (PZT). The fluorescence light from the sample is collected via one of the lenses, separated through a dichroic mirror and focused onto a pinhole placed in front of a photomultiplier tube. The photomultiplier is operated in the photon counting mode.

^{a)} Author to whom correspondence should be addressed.

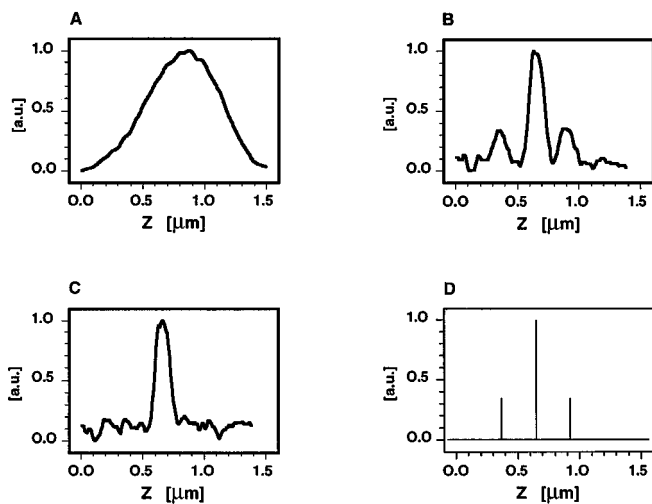


FIG. 2. Axial responses to a subresolution fluorescent layer of a (A) two-photon confocal and (B) two-photon 4Pi confocal microscope. The curves show the axial resolution capability of the two microscopical techniques. The two-photon 4Pi confocal response can be mathematically split into a single peak function (C) and a lobe function (D). (C) is obtained from (B) by convolving with the inverse of the lobe function. The inverse filter is a linear finite response convolution filter with three points and thus can be used on-line when recording 4Pi confocal images. The axial FWHM of the 4Pi confocal response [(B) and (C)] is 140 nm as opposed to 630 nm of the two-photon confocal response (A), showing the fivefold increased axial resolution.

To determine the axial resolution of the 4Pi confocal setup, we recorded axial responses of a subresolution (<50 nm) film of fluorophore (Rhodamine 6G). The fluorophore film was generated by pulsed laser fluorophore deposition (PLFD).¹⁰ Figure 2 shows the response for the (A) two-photon confocal and the (B) two-photon 4Pi confocal microscope. The full width at half-maximum (FWHM) of the two-photon 4Pi confocal response is 140 nm, in contrast to the 680 nm of the normal two-photon confocal response, thus showing the axial resolution potential of the technique. The relative height of the axial lobes for the 4Pi confocal response is 28%. The FWHM of the 4Pi confocal response agrees well with the theoretical prediction, the theoretical value for the lobes is only 15%. In a routine application with index of refraction of the specimen differing from that of the surrounding medium higher lobes are expected. This urges for a solution of the lobe problem.

The rather simple shape of the axial response of the two-photon excitation 4Pi confocal microscope allows the elimination of the effect of the lobes in the image by computational approaches. A fast and efficient computational elimination of the lobes is based on the assumption that the 4Pi response, $h_{4\text{Pi-PSF}}$ consists of the convolution of two functions: the lobe function l [Fig. 2(D)], and the peak function h_{peak} [Fig. 2(C)]. The lobe function is a product of (three) offset δ functions weighted with the height of the ordinary confocal PSF, describing the location of the lobes and their relative height. The peak function quantifies the intensity distribution of a single peak;

$$h_{4\text{Pi-PSF}}(r, z) = l(r, z) \otimes h_{\text{peak}}(r, z). \quad (1)$$

The lobe function and thus the lobes can be computationally removed by multiplying the 4Pi response by the inverse of

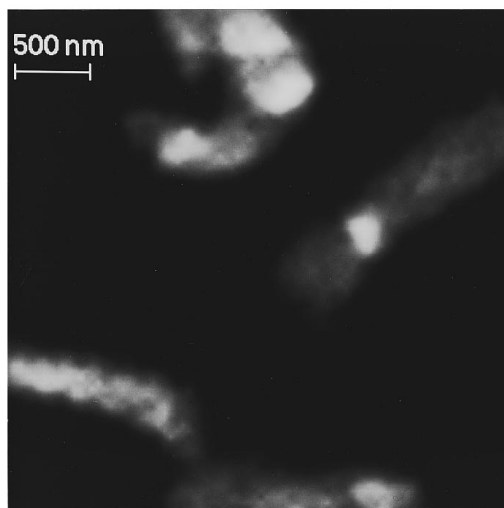


FIG. 3. The chromosome specimen. Overview of DAPI-labeled human lymphocyte chromosomes recorded in the focal plane of the two-photon excitation confocal microscope. (Specimen kindly provided by Dr. T. Cremer, Heidelberg.)

the lobe function in the fourier space. The resulting response is the peak function which is a single peak, namely the main maximum:

$$H_{\text{peak}} = H_{4\text{Pi-PSF}} L^{-1}, \quad h_{\text{peak}} = F^{-1}(H_{\text{peak}}). \quad (2)$$

An efficient approximated spatial inverse filter is a three point filter given by:

$$l_{\text{inv}}(z) = [C_i \delta(z - z_i)] | z_i = \{-d, 0, d\}, \quad C_i = \{-C, 1, -C\}, \quad (3)$$

where C_i are the relative height of the lobes and d the distance between lobes. The inversion of the lobe function is then performed in spatial domain:

$$h_{\text{peak}}(r, z) \approx h_{4\text{Pi-PSF}}(r, z) \otimes l_{\text{inv}}(z), \quad (4)$$

With the object function O , the image from a 4Pi instrument is then

$$I(r, z) = h_{\text{peak}}(r, z) \otimes O(r, z) = [h_{4\text{Pi-PSF}}(r, z) \otimes O(r, z)] \otimes l_{\text{inv}}(r, z). \quad (5)$$

The filter has turned out to perform excellently when the lobes are below 50%. The simple form of Eqs. (4) and (5) allows a rapid on-line application of the filter. According to Eq. (3), the only information that is needed for performing such inverse filtering is the distance between the sidelobes and their relative height. Figure 2(C) presents the effect of this method when a three point filter is applied.

As a next step, we recorded images within a biological sample. We prepared a sample consisting of human lymphocyte chromosomes labeled with DAPI and mounted in glycerol (Fig. 3). We first recorded images of a subresolution point like agglomeration of the fluorophore (Fig. 4). Since the system was no longer aberration-free due to refractive index variations introduced by the sample, the lobes were about 40%.

The effect of the lobes is removed by the three point deconvolution technique as shown in Fig. 4(c). A striking

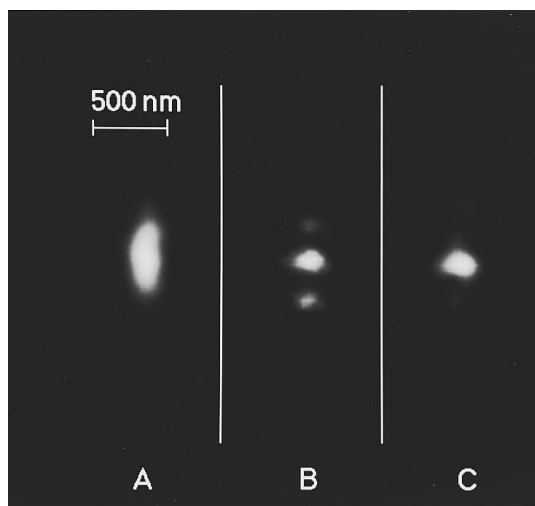


FIG. 4. Axial sections of a point like agglomeration of unbound fluorescent molecules within the specimen. The section shows both the axial and lateral resolution capabilities (A) displays the axial section recorded in the two-photon confocal mode. The axial and lateral extent of the section is 620 and 210 nm, respectively. (B) shows the section recorded in the two-photon 4Pi confocal mode. In (C) the effect of the lobe function of 4Pi confocal sectioning is canceled. The axial and lateral extents of the 4Pi confocal section are 140 and 210 nm, respectively.

difference is observed when comparing Fig. 4(c) with the standard two-photon confocal image [Fig. 4(a)].

As the next step we recorded axial images of DAPI-labeled chromosomes. Figure 5(A) shows the two-photon confocal axial image and Fig. 5(B) its 4Pi confocal counterpart with the three point deconvolution. The two images show an axial cut through two objects a and b. In Fig. 5(A) the objects seem to be extended along the optical axis. Furthermore from the confocal image it is not apparent if object a has lower concentration of bound label, if it is out of focus or if it is smaller than object b. In Fig. 5(B) the 4Pi confocal section from the same position is shown. The objects in Fig. 5(B) are localized axially with an accuracy of 140 nm. It is also apparent that the smaller amount of fluorescence signal in Fig. 5(A) was due to the fact that the subresolution object a is smaller than object b.

From the results it is apparent that two-photon 4Pi con-

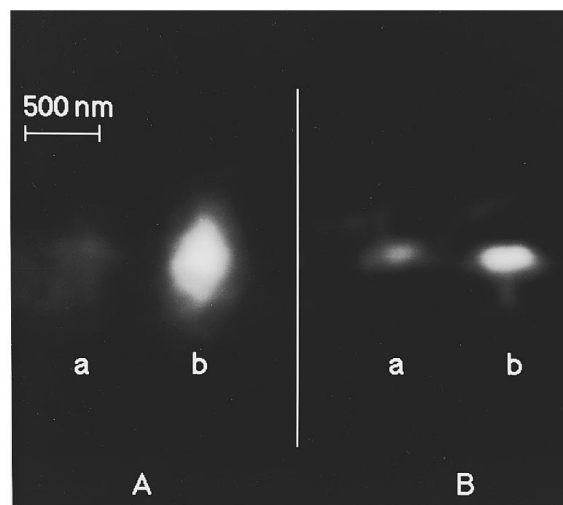


FIG. 5. Axial sectioning of DAPI-labeled human lymphocyte chromosomes. The two-photon confocal axial image is displayed in (A) whereas its 4Pi confocal counterpart is shown in (B) after cancellation of the lobe function. The images feature axial section through two objects (a) and (b). In the two-photon confocal image in (A) the objects seem to be extended 630 nm along the optical axis. The objects (B) are localized axially with an accuracy of 140 nm in the 4Pi confocal mode.

focal microscopy has reached a level where it can be applied to microscopical research of biological specimens. The fourfold to fivefold increase in axial resolution as compared to its standard confocal counterpart can be exploited in high resolution studies of subcellular organelles and their structure.

This work was supported by the Academy of Finland.

¹S. Hell and E. H. K. Stelzer, *J. Opt. Soc. Am. A* **9**, 2159 (1992).

²S. Hell and E. H. K. Stelzer, *Opt. Commun.* **93**, 277 (1992).

³C. J. R. Sheppard and C. J. Cogswell, *Optics in Medicine, Biology and Environmental Research*, edited by G. v. Bally (Elsevier, Amsterdam, 1993), pp. 310–315.

⁴S. W. Hell, S. Lindek, C. Cremer, and E. H. K. Stelzer, *Appl. Phys. Lett.* **64**, 1335 (1994).

⁵F. Lanni, *Application of Fluorescence in the Biological Sciences*, edited by D. L. Taylor (Liss, New York, 1986), pp. 505–521.

⁶B. Bailey, D. L. Farkas, D. L. Taylor, and F. Lanni, *Nature* **366**, 44 (1993).

⁷F. Lanni, B. Bailey, D. L. Farkas, and D. L. Taylor, *BioImaging* **1**, 187 (1994).

⁸S. W. Hell, S. Lindek, and E. H. K. Stelzer, *J. Mod. Opt.* **41**, 675 (1994).

⁹M. Gu and C. J. R. Sheppard, *Opt. Commun.* (in press).

¹⁰S. W. Hell, A. Utz, P. Hänninen, and E. Soini (unpublished).